J. Astrophys. Astr. (2002) **23,** 213–233

Fast Transition between High-soft and Low-soft States in GRS 1915 + 105: Evidence for a Critically Viscous Accretion Flow

S. Naik[1], A. R. Rao[1] & Sandip K. Chakrabarti[2]

[1] *Tata Institute of Fundamental Research, Homi Bhabha Road, Mumbai, 400 005, India.*
[2] *S. N. Bose National Center for Basic Sciences, Salt Lake, Calcutta, 700 091, India.*

Abstract. We present the results of a detailed analysis of RXTE observations of class ω (Klein-Wolt *et al.* 2002) which show an unusual state transition between high-soft and low-soft states in the Galactic microquasar GRS 1915 + 105. Out of about 600 pointed RXTE observations, the source was found to exhibit such state transition only on 16 occasions. An examination of the RXTE/ASM data in conjunction with the pointed observations reveals that these events appeared as a series of quasi-regular dips in two stretches of long duration (about 20 days during each occasion) when hard X-ray and radio flux were very low. The X-ray light curve and colour-colour diagram of the source during these observations are found to be different from any reported so far. The duration of these dips is found to be of the order of a few tens of seconds with a repetition time of a few hundred seconds. The transition between these dips and non-dips which differ in intensity by a factor of ~ 3.5, is observed to be very fast ($\sim$ a few seconds). It is observed that the low-frequency narrow QPOs are absent in the power density spectrum (PDS) of the dip and non-dip regions of class ω and the PDS is a power law in the 0.1 – 10 Hz frequency range. There is a remarkable similarity in the spectral and timing properties of the source during the dip and non-dip regions in this set of observations. These properties of the source are distinctly different from those seen in the observations of other classes. This indicates that the basic accretion disk structure during both dip and non-dip regions of class ω is similar, but differ only in intensity. To explain these observations, we invoke a model in which the viscosity is very close to critical viscosity and the shock wave is weak or absent.

Key words. Accretion, accretion discs — binaries: close — black hole physics — stars: individual: GRS 1915 + 105 — X-rays: stars

1. Introduction

The Galactic microquasar GRS 1915 + 105 was discovered in 1992 with the WATCH instrument on-board the GRANAT satellite (Castro-Tirado *et al.* 1992). Subsequent radio observations led to the identification of a superluminal radio source at a distance of 12.5 ± 1.5 kpc ejecting plasma clouds at $v \sim 0.92c$ (Mirabel & Rodriguez 1994). Since the discovery, the source has been very bright in X-rays, emitting at a luminosity of more than 10^{39} erg s^{-1} for extended periods. It exhibits peculiar types of X-ray

variability characteristics (Greiner *et al.* 1996) which have been interpreted as the instabilities in the inner accretion disk leading to the infall of matter into the compact object (Belloni *et al.* 1997). Strong variability is observed in X-ray, radio and infrared over a wide range of time scales. Observations with the Burst and Transient Source Experiment (BATSE) on the *Compton Gamma Ray Observatory* have revealed the highly variable nature of the source in the hard X-rays. The intensity variations of as much as 3 Crab have been observed on time scales from seconds to days (Muno *et al.* 1999). The X-ray emission is characterized by quasi-periodic oscillations (QPOs) at centroid frequencies in the range of 0.001–67 Hz (Morgan *et al.* 1997). It is found that the intensity dependent narrow QPOs are a characteristic property of the low-hard state (Chen *et al*. 1997). Based on extensive X-ray studies, Muno, Morgan & Remillard (1999) classified the behavior of the source into two distinct states, spectrally hard-state with the presence of narrow QPOs, dominated by a power-law component and the soft-state with the absence of QPOs, dominated by thermal emission. Attempts have been made to connect the observed radio characteristics in GRS $1915+105$ like jets and superluminal motion with the X-ray emission from the accretion disk (Naik & Rao 2000; Naik *et al.* 2001 and references therein). They have interpreted the observed soft dips in the X-ray light curves of the source as the evacuation of matter from the accretion disk and superposition of a series of such dip events produce huge radio flares in the source.

An extensive study of all the publicly available RXTE pointed observations from 1996 January to 1997 December lead to a classification into 12 different classes on the basis of structure of the X-ray light curve and the nature of the colour-colour diagram (Belloni *et al.* 2000). According to this classification, the source variability is restricted into three basic states, a low-hard state with invisible inner accretion disk (C), a high-soft state with visible inner accretion disk (B) and a low-soft state with spectrum similar to the high-soft state and with much less intensity (A). Belloni *et al.* (2000) suggested that the state transition between two canonical states (B and C) takes place through a hint of state A. During the transition between low-hard (C) and high-soft (B) states, the source shows the properties of state A for a duration of about a few seconds. Longer duration (≥ 20 s) of state A (soft-dip) has been observed during the transition from low-hard state to high-soft state in class β (after the spike in the X-ray light curve) and in the observations of class θ when the source exhibits the properties of low-hard state (C) during the non-dip regions. Recently, Klein-Wolt *et al.* (2002) have discovered an unusual state transition between high-soft and low-soft states in the microquasar GRS $1915+105$. This type of transition between two different intensity states was not observed in any other black hole binaries. The low-soft state (state A) is a rare occurrence in Galactic Black hole sources. In GRS $1915+105$ it appears briefly (for a few seconds) during the rapid state transition between states C and B as well as during the soft dips seen during the variability classes β and θ (in the nomenclature of Belloni *et al.* 2000), which are associated with high radio emission (Mirabel *et al.* 1998; Naik & Rao 2000; Naik *et al.* 2001). On rare occasions, long stretches of state A are also seen in this source (the variability class ϕ). Recently, Smith *et al.* (2001) reported a sudden transition from a spectrally hard state to soft state with much lower intensity in GRS $1758-258$. Though transition from low-hard to high-soft states are seen in many Galactic black hole candidate sources, a transition between two different intensity states (high and low) with similar physical parameters of the accretion disk was not observed in GRS $1915+105$ or in any other black hole binaries.

The extremely variable nature of the microquasar GRS 1915 + 105 is restricted within three canonical spectral states A, B, and C. (as described above). The source is observed to be in spectral state C, (low-hard state) for wide time ranges starting from hundreds of seconds to tens of days to a few months whereas the source remains in the spectral state B, (high-soft state) only for a few occasions (Rao *et al.* 2000). These properties are also seen in other Galactic black hole binaries. The broad-band spectra of the source obtained from the observations with the Oriented Scintillation Spectroscopy Experiment (OSSE) aboard the *Compton Gamma Ray Observatory* along with the simultaneous observations with RXTE/PCA during lowest X-ray fluxes (low-hard state C; 1997 May 14 – 20) and highest X-ray fluxes (high-soft state B; 1999 April 21 – 27) are well fitted by Comptonization of disk blackbody photons in a plasma with both electron heating and acceleration (Zdziarski *et al.* 2001). Although the RXTE/PCA observation during 1999 April 21 – 27 is of class γ which is not a pure high-soft state B rather a combination of states A and B, the overall spectrum is dominated by the high-soft state B. During the above period, the hard X-ray photon flux in 20 – 60 keV energy range with BATSE is also found to be very low ($\sim$ 0.03 photons cm^{-2} s^{-1}) which indicates the source spectrum to be soft. On a careful analysis of the RXTE/PCA observations which show high frequency QPO with constant centroid frequency of 67 Hz, arising in the inner accretion disk of the black hole binary (Morgan *et al.* 1997), it is found that these observations are of classes λ, μ, γ. δ with spectral state of high-soft state B. As these properties are associated with the inner accretion disk of the black hole, it is interesting to study the RXTE/PCA observations during the high-soft states with low value of hard X-ray photon flux with BATSE in detail.

In this paper, we present the evidence of fast transitions between two different X-ray intensity states with similar spectral and timing properties in GRS 1915 + 105. A detailed spectral and timing analysis is presented which shows that the low-soft state is very different from the spectral state A seen during other variability classes. We have tried to explain the observed peculiar state transition in GRS 1915 + 105 on the basis of the presence of an accretion disk with critical viscosity which causes the appearance and disappearance of sub-Keplerian flows out of Keplerian matter.

2. Analysis and results

We have made a detailed examination of all the publicly available RXTE pointed observations on GRS 1915 + 105 in conjunction with the continuous monitoring of the source using RXTE/ASM. Based on the X-ray light curve and the hardness ratio, we could identify most of the pointed observations into the 12 variability classes suggested by Belloni *et al.* (2000), and associate the global properties of the source with other characteristics like radio emission (see Naik & Rao 2000). During these investigations a new variability class was found to be occurring during two time intervals, 1999 April 23 – May 08 (MJD 51291–50306) and 1999 August 23 – September 11 (MJD 51410–51432), respectively. This new class which is called as class ω (Klein-Wolt *et al.* 2002), was observed in a total of 16 pointed RXTE observations and is characterized by a series of dips of duration of 20–95 s and repetition rate of 200–600 s.

To compare and contrast the X-ray properties of the source during this new class with other reported classes, we show, in Fig. 1, the X-ray light curve of the source obtained with RXTE/ASM in 1.3 – 12.1 keV energy range (top panel) with the hard X-rays photon flux in 20 – 60 keV energy range (bottom panel). The data for hard

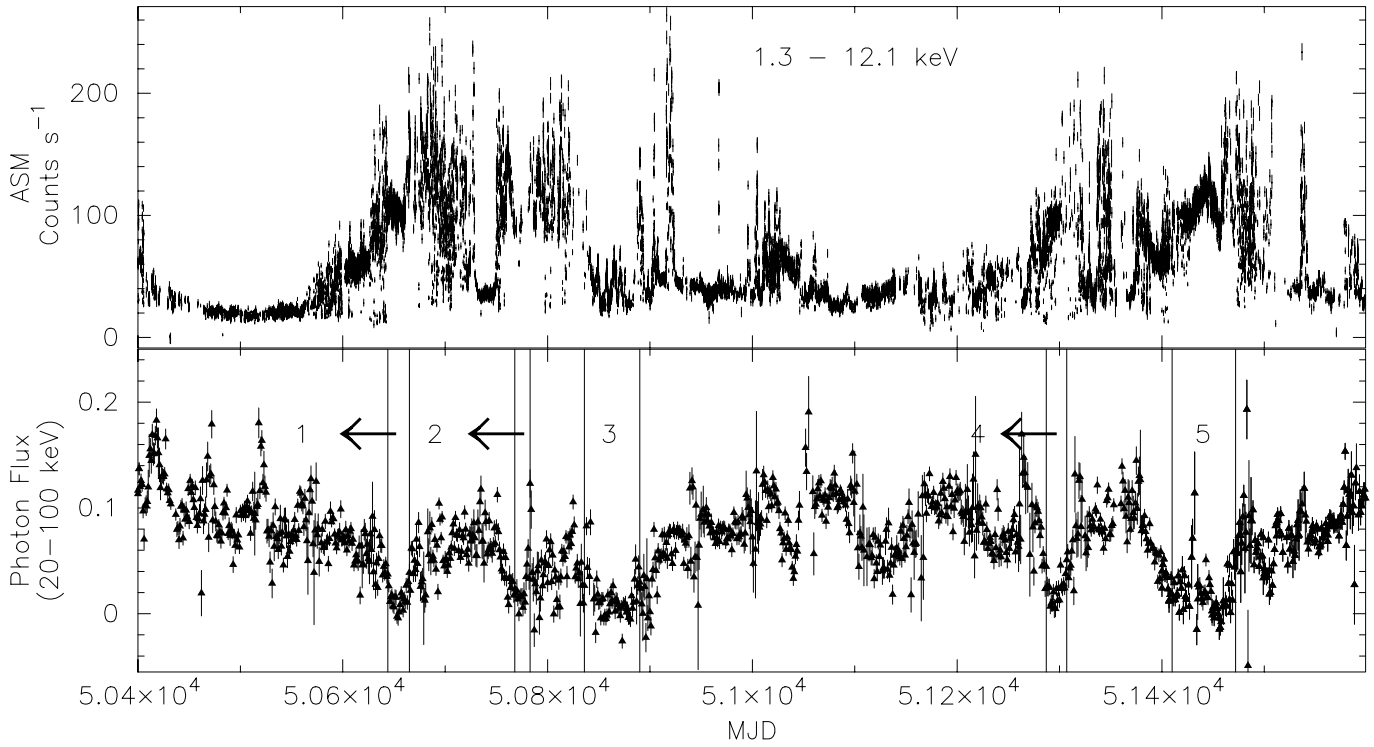

Figure 1. The X-ray light curve for GRS 1915 + 105 with RXTE/ASM in the energy range 1.3 – 12.2 keV is shown in the upper panel with the hard X-ray photon flux in the energy range 20 – 60 keV with BATSE in the bottom panel. The regions (1), (2), (3), (4), and (5) in the bottom panel indicate the presence of the long duration ($\geq$ 10 days) soft-spectral states of the source when the hard X-ray photon flux of the source is $\sim$ 0.03 photons cm^{-2} s^{-1}.

X-rays were taken from the Burst and Transient Source Experiment (BATSE) on the *Compton Gamma Ray Observatory*. We have selected the time range (MJD 50400 – 51600) during which the X-ray (1.3 – 12.1 keV), radio and hard X-ray (20 – 60 keV) data are available. We have selected five regions of durations of more than about 10 days when the hard X-ray photon flux is ~ 0.03 photons cm^{-2} s^{-1}. These regions are marked by vertical lines in the bottom panel of Fig. 1.

To examine the variation in the source flux at different energy bands (X-ray, radio, and hard X-ray photon flux), we have plotted in Fig. 2, the ASM light curve in 1.3 – 12.2 keV energy range (top panel), radio flux density at 2.25 GHz (middle panel), and the hard X-ray photon flux (bottom panel) during above five different regions. The start time of RXTE pointed observations during these five intervals and the class (Belloni *et al*. 2000) to which these observations belong to, are marked in the bottom panel of the figure. The average ASM count rate, average flux density at 2.25 GHz, spectral index and the hard energy photon flux during all these five regions are given in Table 1. From the table, it is observed that the average ASM count rate during first, second and fifth regions are $\sim$ 100 counts s^{-1} and $\sim$ 80 counts s^{-1} during fourth region whereas the count rate is too low ($\sim$ 40 counts s^{-1}) during the third region. It is observed that the rms variation in the source count rate is maximum during the third region. However, the radio flux density at 2.25 GHz and the hard X-ray photon flux are found to be indifferent during all these five intervals. From a careful analysis of the RXTE pointed observations during these five intervals, it is found that the RXTE observations are of class γ (regions 1, 2, and two observations in region 3), class ϕ (region 3), class δ (half of the region 5) and class ω (new class; regions 4 and 5). These observations and the classes are indicated in the bottom panel of Fig. 2. The X-ray light curves of the RXTE pointed observations in 1999 April – May and 1999 August – September (class ω) which show a quasi-regular and distinct transition between two different X-ray intensity states (dip and non-dip) are different from the reported 12 different classes.

Out of about 600 RXTE pointed observations, there are only 16 occasions when the source shows the unusual transition between two different intensity states (class ω). We emphasize here that these 16 observations occur only during two occasions (51290 – 50306 and 51410 – 51433 MJD ranges) when the hard X-ray flux was low (as described above). We have shown, in Fig. 3, the X-ray light curve for one such observation carried out on 1999 April 23 (Obs. ID: 40403-01-07-00). The panel (a) in the figure shows the RXTE/PCA light curve of the source in 2 – 60 keV energy band (normalized to 5 Proportional Counter Units (PCUs)) whereas the panels (b) and (c) show the hardness ratios HR1 (the ratio between the count rate in the energy range 5 – 13 keV to that in 2 – 5 keV) and HR2 (the ratio between the count rates in the energy range 13 – 60 keV and 2 – 13 keV), respectively. In panels (d), (e), and (f), we have shown the source light curves (normalized to 5 PCUs) in 2 – 5 keV, 5 – 13 keV, and 13 – 60 keV energy bands respectively. The average value of source count rate in different energy bands during the dip, non-dip, and the total light curves are given in Table 2 along with the hardness ratios HR1 and HR2. From Fig. 3 and Table 2, it can be seen that the variability in the source flux is low during the dips in all the energy bands. It is, however, observed that the source variability decreases at high energy bands. An intensity difference by a factor of ≥ 3 is observed between the non-dip and dip regions at low energy bands which ~ 2 at hard X-ray bands. This indicates that the change in the source flux during dip and non-dip regions are significant in soft X-

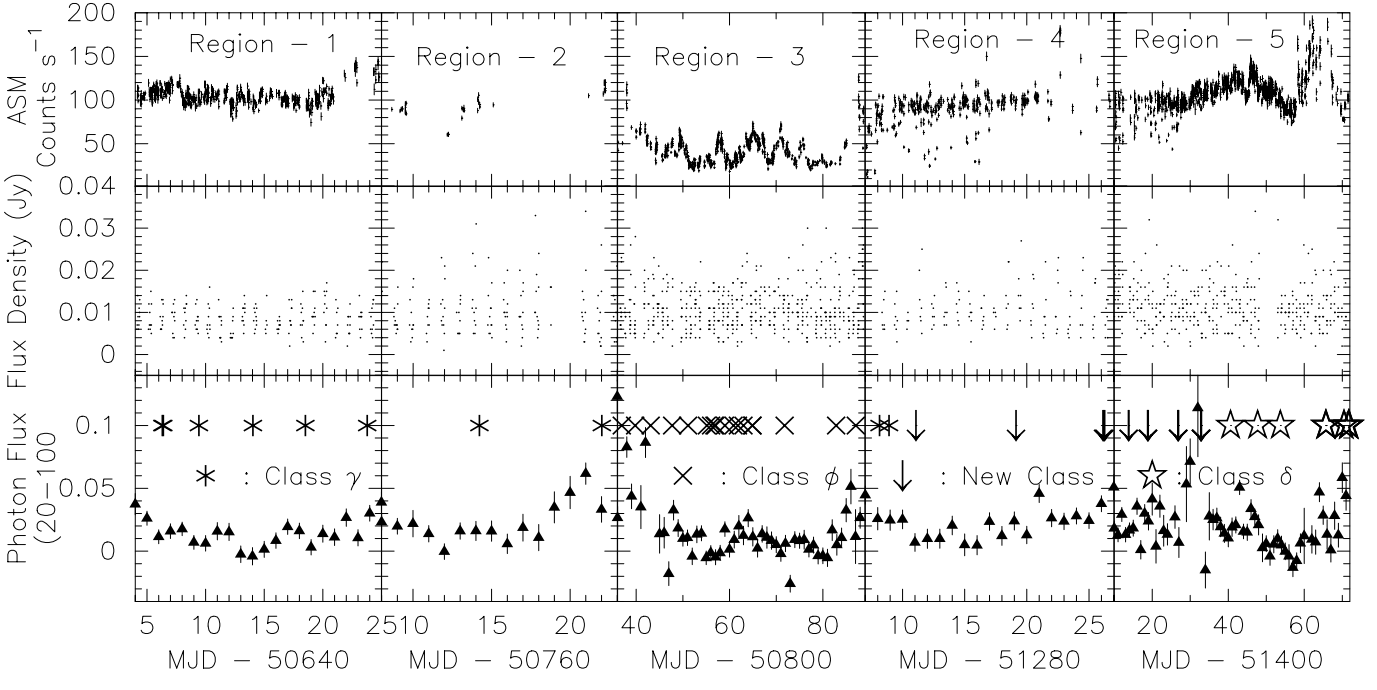

Figure 2. The X-ray light curve for GRS 1915 + 105 with RXTE/ASM in the energy range 1.3–12.2 keV during the 5 different regions marked in Fig. 1 (bottom panel) is shown in the upper panel with the radio flux at 2.25 GHz (second panel) and hard X-ray photon flux in the energy range 20 – 60 keV with BATSE (bottom panel). The start time of RXTE pointed observations during these five intervals are indicated by different markers in the bottom panel of the figure.

Table 1. Statistics of five different regions shown in Fig. 2.

	Region – 1	Region – 2	Region – 3	Region – 4	Region – 5
ASM Count rate[1]	103.4 ± 2.8	91.3 ± 6.7	37.6 ± 7.4	78.9 ± 11.7	102.8 ± 6.5
Flux density[2]	0.009 ± 0.0002	0.011 ± 0.0006	0.011 ± 0.0002	0.011 ± 0.0005	0.011 ± 0.0003
Spectral Index	-0.11 ± 0.05	-0.15 ± 0.06	-0.25 ± 0.03	-0.06 ± 0.06	$+0.07 \pm 0.04$
Photon flux[3]	0.014 ± 0.002	0.022 ± 0.006	0.009 ± 0.003	0.023 ± 0.003	0.018 ± 0.002

[1] The average ASM count rate obtained from the Dwell data and the quoted errors are the rms deviations from the average count rate.
[2] Flux density in mJy at 2.25 GHz.
[3] Hard X-ray flux from BATSE in photons cm^{-2} s^{-1}.

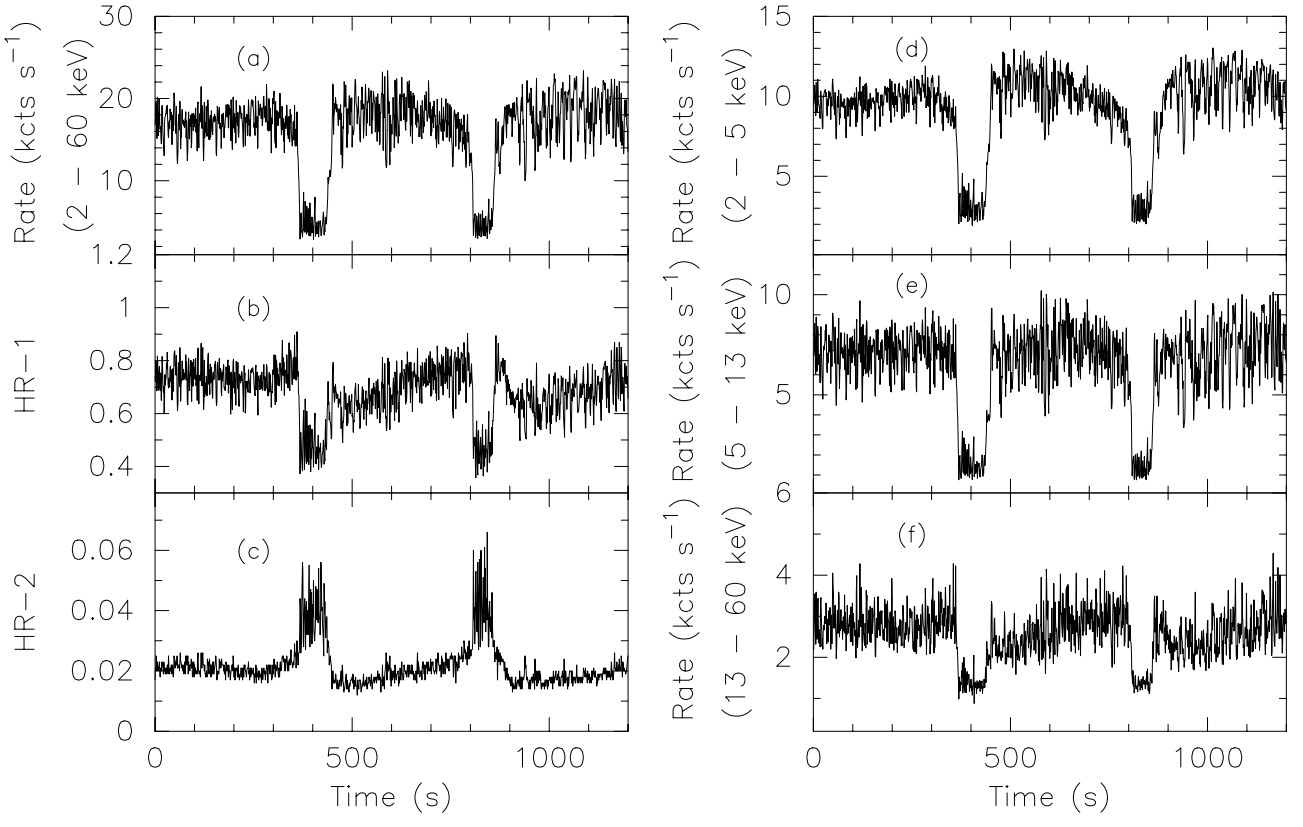

Figure 3. Light curve (2 – 60 keV energy range for 5 PCUs) of GRS 1915 + 105 for the RXTE/PCA pointed observation on 1999 April 23 (new class ω) is shown along with the hardness ratios HR1 (count rate in 5 – 13 keV / count rate in 2 – 5 keV energy range) and HR2 (count rate in 13 – 60 keV / count rate in 2 – 13 keV energy range). The light curves at 2 – 5 keV, 5 – 13 keV, and 13 – 60 keV energy bands are shown in the right panels. Low values of HR1 ($\leq$ 1.0) and HR2 ($\leq$ 0.06) indicate the softness of the spectrum during both the dip and non-dip regions.

Table 2. Statistics of the non-dip and dip regions shown in Fig. 3.

Energy range	Average count rate[1]			Flux
(in keV)	Non-dip region	Dip region	Total (dip and non-dip)	Ratio[2]
$2-5$	9744 ± 46	3171 ± 95	8991 ± 68	3.1 ± 0.1
$5-13$	7147 ± 55	1593 ± 78	6298 ± 57	4.5 ± 0.22
$13-60$	2787 ± 23	1393 ± 29	2511 ± 17	2.0 ± 0.05
$2-60$	17239 ± 101	4938 ± 175	15603 ± 125	3.5 ± 0.13

[1] Average count rate (in counts s^{-1}).
[2] Ratio between the average count rate during the non-dip region to the dip region.

ray bands which decreases significantly in hard X-ray bands. The low intensity dips are characterized by HR1 and HR2 in 0.35 – 0.55 and 0.03 – 0.06 ranges respectively whereas the non-dip regions are characterized by HR1 and HR2 in 0.6 – 0.8 and 0.15 – 0.25 ranges respectively. The observed differences between the hardness ratios HR1 and HR2 during the dip and non-dip regions are not significant enough to highlight the difference in the spectral properties of the source.

The duration of the dips in the light curves of all the 16 RXTE pointed observations of class ω which show the unusual transition between two different intensity states, lies in the time range of 20 – 95 s whereas the non-dip regions last for 200 – 525 s. Although the duration of the dips was high in the beginning of the observations during both the occasions, sparse RXTE pointed observations restrict us to present any statistical picture of the duration and the repetition period of these dips. Figure 3 shows that the HR1 is low during the dips.

To study the timing properties of the source, we have generated the power density spectrum (PDS) in 2 – 13.1 keV energy band for the dip (low intensity state) and non-dip (high intensity state) regions of all 16 selected RXTE/PCA pointed observations. It is found that the low frequency narrow QPOs are absent in the PDS of both dip and non-dip regions of all the observations. We have fitted the PDS of both the dips and non-dip regions with a power-law in frequency ranges 0.1 – 1 Hz and 1 – 10 Hz. It is found that there is no significant difference in the power law index during both the intensity states. The only distinguishing feature of the two intensity states is the higher rms variability in both the frequency bands during the low intensity (dip) state compared to the high intensity (non-dip) state. Figure 4 shows the PDS of the two different regions of the RXTE/PCA pointed observation on 1999 April 23. From the figure, it is found that the PDS during both the regions are a featureless power law in 0.1 – 10 Hz range.

We have attempted a wide band X-ray spectroscopy of the dip and non-dip regions of the RXTE observation of the source on 1999 August 23 (Obs. ID : 40703-01-27-00). The data for the dip region were selected when the source count rate was less than ≤ 3000 counts s^{-1} (for 2 PCUs) in 2 – 60 keV energy range and non-dip region when the count rate was ≥ 5000 counts s^{-1}. We have generated 128 channel energy spectra from the standard 2 mode of the PCA and 64 channel spectra from HEXTE for the dip and non-dip regions. Standard procedures for data selection, background estimation and response matrix generation have been applied. Systematic error of 2% has been added to the PCA spectral data. We have used the archive mode data from

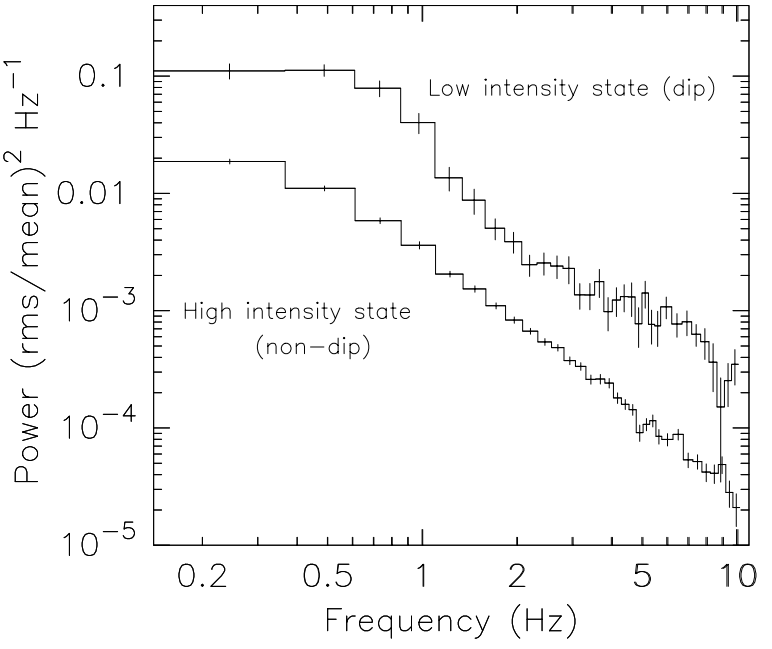

Figure 4. PDS of the source GRS 1915 + 105 in the energy range of 2 – 13 keV for high-soft and low-soft states of the X-ray light curve obtained from RXTE/PCA on 1999 April 23. The absence of the narrow QPO in the frequency range of 0.1 – 10 Hz is clear. The normalized power at a given frequency is high for the low-soft (dip) state and is low for the high-soft state (non-dip).

Cluster 0 of HEXTE for better spectral response. The spectra were re-binned at higher energy band to fewer number of channels in order to improve the statistics. 3 – 50 keV energy range PCA data and 15 – 180 keV energy range HEXTE data are used for spectral fitting. The dip and non-dip spectra are fitted with the standard black hole models (Muno *et al.* 1999) consisting of "disk-blackbody and a thermal-Compton spectrum", "disk-blackbody and a power-law", and "disk-blackbody, a power-law and a thermal-Compton spectrum" with a fixed value of absorption by intervening cold material parameterized as equivalent hydrogen column density, N_H at 6×10^{22} cm^{-2}. From the spectral fitting, it is observed that the model with disk-blackbody, a power-law, and a thermal-Compton spectrum as model components fits very well with the data during both the dip and non-dip regions. It is observed that the source spectrum is similar in hard X-ray energy bands ($\geq$ 50 keV) for both the dip and non-dip regions. The fitted parameters for the best fit model during two different regions along with the 2 – 50 keV source flux for each model components are given in Table 3. Assuming the distance of the source as 12.5 kpc, we have calculated the luminosity of the source in 3 – 60 keV energy band to be $\sim 7.83 \times 10^{38}$ ergs s^{-1} and 2.2×10^{38} ergs s^{-1} for non-dip and dip regions respectively. The parameters in the table show the similarities in the properties of the accretion disk during two different intensity states. From the results of the spectral fitting, we found that the spectrum of the source is soft with similar parameters of the accretion disk during both the different intensity states. We have shown, in Fig. 5, the energy spectra obtained from the RXTE/PCA and HEXTE observations of the source with the fitted model ("disk-blackbody, a power law and a thermal Compton spectrum) during two different intensity states. The upper panel in

Table 3. Spectral parameters during high-soft and low-soft states of class ω of GRS 1915 + 105 for the model "disk-blackbody, a power law and a thermal Compton spectrum".

X-ray intensity state	Reduced χ^2	$kT_{\rm in}^1$ (keV)	kT_e^2 (keV)	Γ_x^3	Inner disk radius (km)	L^4 ergs s^{-1}
High-soft (non-dip)	0.68 (76 dof)	$1.7^{+0.05}_{-0.06}$	$2.5^{+0.13}_{-0.15}$	$2.9^{+0.2}_{-0.97}$	42^{+5}_{-3}	7.83×10^{38}
Low-soft (dip)	0.68 (66 dof)	$1.55^{+0.03}_{-0.05}$	$4.05^{+0.042}_{-0.045}$	$2.03^{+0.1}_{-0.1}$	25^{+6}_{-3}	2.2×10^{38}

[1] kT_{in} : Inner disk temperature.
[2] kT_e : Temperature of the Compton cloud.
[3] Γ_x : Power-law photon index.
[4] L : Luminosity of the source in 3 – 60 keV energy range, assuming the distance of the source to be 12.5 kpc.

Fig. 5 shows the the energy spectrum and the best fit model for the non-dip region of class ω whereas the bottom panel shows the spectrum and the fitted model for the dip regions. From the figure, it is observed that the dip and non-dip spectra are dominated by the thermal component.

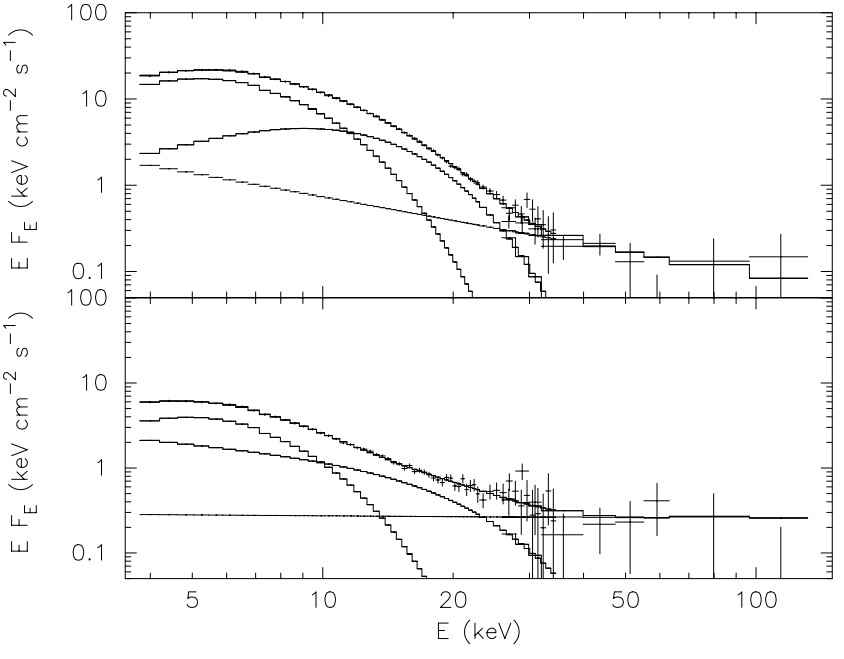

Figure 5. The observed count rate spectrum of GRS 1915 + 105 during high-soft (non-dip) and low-soft (dip) states of the new class ω obtained from RXTE/PCA and HEXTE data. A best-fit model consisting of a disk blackbody, a power-law, and a thermal Compton spectrum is shown as histogram with the data.

In order to investigate the structure of the inner accretion disk during the observed unusual transition between two different intensity states, we have calculated the characteristic radius of the inner disk ($R_{col} = D_{10\,\mathrm{kpc}}\sqrt{N_{bb}/cos\theta}$) from the normalization parameter of the disk blackbody (N_{bb}). Assuming the distance of the source to be 12.5 kpc ($D_{10\,\mathrm{kpc}} = 1.25$), and an inclination angle (θ) equal to that of the radio jets, 70°, the radius of the inner accretion disk is found to be 41 ± 7 km during the non-dip (high intensity state) and 25 ± 3 km during the dip (low intensity state) regions. The temperature of the inner accretion disk during the dip and non-dip regions are found to be 1.54 and 1.72 keV respectively. Using these values, we have estimated the ratio of the total flux from the disk ($F_{bb} = 1.08 \times 10^{11} N_{bb}\sigma T_{col}^4 \mathrm{ergs}^{-1}\mathrm{cm}^{-2}$ s, where σ is the Stephan-Boltzmann constant) during non-dip and dip regions to be ~ 3.9 which is observed from the X-ray light curves. From this analysis, we conclude that the observed transition between the different intensity states is associated with the change in temperature of the inner accretion disk without any change in the radius.

3. Comparison between various spectral states

The spectral and temporal properties of the source were studied by Rao *et al*. (2000) when the source was making a slow transition from a low-hard state (C) to a high-soft state (B) in about three months. Rapid state transitions between the above two canonical spectral states were also observed when the source was exhibiting a series of fast variations, which can be classified as bursts (Rao *et al*. 2000). It was pointed that the spectral and timing properties of the source during the short duration B and C states are identical to those seen during the long duration B and C states. Fast transition between low-hard (C) and low-soft states (A) was also observed when the light curve of the source contains a series of X-ray soft dips (Naik *et al*. 2001). Although Belloni *et al*. (2000) have classified the RXTE/PCA observations of low-hard states into four different sub-classes ($\chi 1$, $\chi 2$, $\chi 3$, and $\chi 4$), there is not much difference in the temporal and spectral properties of the source during the observations of these four sub-classes. During the observations of class ϕ, the source remains in low-soft state (A) whereas during all other classes, it is observed that the source remains in high-soft spectral state (B) or makes transition between the spectral states B and C, and C and A. Although the transition between the spectral states B and A is seen during the observations of a few classes, the duration of the spectral state A is in the order of a few seconds. However, the transition between the states A and B as observed during the observations of class ω where the source remains in state A for a few tens of seconds is different. As both the spectral states A and B are characterized by the soft spectrum with inner accretion disk extending towards the black hole event horizon, the difference in the observed transition between these two states needs a detailed comparison between these three states along with the low-soft state observed during the class ω.

According to the Belloni *et al*. (2000) classification, the source variability ranges from a steady emission for long durations like in classes ϕ, χ to large amplitude variations in classes λ, κ, ρ, α. Short periodic flickering with different amplitudes is seen during the observations of classes γ, μ and δ. During the observations of classes θ, β, and ν, the amplitude variation is accompanied by soft X-ray dips with duration of a few tens of seconds to hundreds of seconds. It is observed that the properties of the source during the observations of class α are similar to those during the combined classes ρ and χ (Naik *et al*. 2002). However, the RXTE pointed observations which

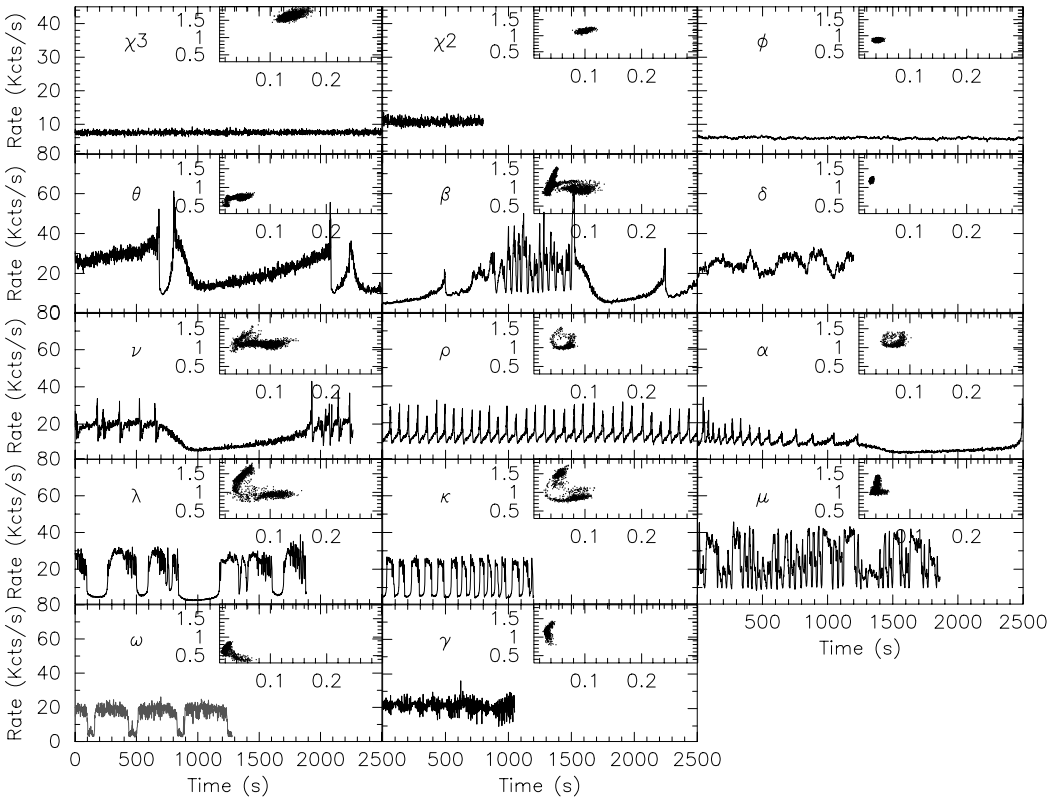

Figure 6. X-ray light curves (2 – 60 keV energy range) and colour-colour diagram (HR1 vs HR2) of GRS 1915 + 105 for observations of all classes (Belloni *et al.* 2000) are shown along with the observation of class ω. The insets in each figure shows the colour-colour diagram, HR1 in the Y-axes and HR2 in the X-axes (see text). The Obs. Ids of the data used are $\chi 3$: 20402-01-50-01, $\chi 2$: 20402-01-04-00, ϕ : 30703-01-08-00, θ : 40702-01-03-00, β : 20402-01-44-00, δ : 20402-01-42-00, ν : 10408-01-41-00, ρ : 20402-01-03-00, α : 20402-01-28-00, λ : 20402-01-37-01, κ : 20402-01-33-00, μ : 20402-01-45-01, ω : 40403-01-07-00, and γ : 20402-01-40-00.

show the unusual transition between two different intensity states (class ω) are found to be different from all the other classes. The absence of strong variability in the X-ray light curve, the presence of soft-dips with similar spectral properties as the non-dip regions prompted to investigate the similarities/differences in the source properties during various low and high intensity states with little variability in the X-ray light curve of the reported 12 different classes of RXTE observations.

We have selected one RXTE observation from all the X-ray classes and, in Fig. 6, we have shown the light curves and colour-colour (HR1 vs HR2) diagram of the selected observations. From the figure, it is observed that observations of classes ϕ, δ and ω are characterized by the absence of strong variability in the light curve with HR1 ≤ 1 and HR2 ≤ 0.06 which indicate the softness of the spectrum of the source. Although the observations of classes $\chi 2$ and $\chi 3$ also show less variability in the X-ray light curves, the spectrum of the source is hard with HR1 ≥ 1 and HR2 ≥ 0.1. Comparing the structure of the light curves and colour-colour diagram of all these observations, it is found that the observations which show the unusual intensity transition (class ω) is different from the observations of other classes. We have examined the uncertainty in the value of HR1 (about 0.3) due to the different gains of PCUs at different epochs. But the general trend in the hardness ratios remain unaffected by the change in gains.

To study the spectral properties of the source during these different classes, we have attempted a wide band X-ray spectroscopy of all the RXTE observations which show a gradual change from a high-soft to low-hard state and characterized by a sharp soft dip with low variability (β and θ) and observations which show steady behavior during the orbit of RXTE ($\chi 2$, $\chi 3$, ϕ, and δ) along with one of the observation showing the unusual state transition (class ω). We have selected the radio-quiet low-hard state of class $\chi 2$, radio-loud low-hard state of class $\chi 3$, and the high-soft (non-dip) state of the observations of class ω. Standard procedures for data selection, background estimation and response matrix generation have been applied. We have used the data in the same energy range such as 3 – 50 keV energy range PCA data and 15 – 180 keV energy HEXTE data for spectral fitting. The spectra of all three different classes of observations are fitted with all the three models which were used for the dip and non-dip regions (described in the previous section). The fitted parameters for different models are given in Table 4. Examining the parameters in the table, it is found that "disk-blackbody and a thermal-Compton spectrum" model is suitable for the radio-quiet low-hard state (class $\chi 2$) and "disk-blackbody, a power-law and a thermal-Compton spectrum" model is suitable for the radio-loud low-hard state (class $\chi 3$) and the high state (non-dip) of the observations which show the unusual transition between two intensity states.

To compare the deviations of the spectral parameters of the source during the various low state observations with the above described three well fitted models for the observations of classes $\chi 2$, $\chi 3$, and the non-dip region of the observation showing the peculiar state transition, we analyzed the source spectrum during various dips observed in other classes of RXTE observations along with a few low variability high-state observations of classes ϕ and δ. We have selected data for the low-hard dip of class β (before the spike in the light curve), low-soft dip of class θ which is identical to the dip observed (after the spike) in the light curve of class β, low-intensity observation of class ϕ and high-soft state of class δ. To investigate the similarities in the spectral properties of the source during the above X-ray observations, we have used

Table 4. Spectral parameters during classes $\chi 2$, $\chi 3$, and ω (non-dip) of GRS 1915+105.

X-ray class	Reduced χ^2	$kT_{\rm in}^1$ (keV)	kT_e^2 (keV)	τ^3	Γ_x^4	Count rate HEXTE	Count rate PCA
Model: Disk blackbody + thermal-Compton spectrum							
$\chi 2$ (RQ[5])	1.353	1.348	20.01	3.047	– – –	62.58	4093
$\chi 3$ (RL[6])	8.26	4.068	12.54	4.159	– – –	78.22	4902
ω (High state)	2.035	2.056	4.415	6.489	– – –	71.08	8547
Model: Disk blackbody + power-law							
$\chi 2$ (RQ)	5.313	0.156	– – –	– – –	2.519	– – –	– – –
$\chi 3$ (RL)	33.24	0.156	– – –	– – –	2.636	– – –	– – –
ω (High state)	2.505	2.205	– – –	– – –	3.457	– – –	– – –
Model: Disk blackbody + power-law + thermal-Compton spectrum							
$\chi 2$ (RQ)	1.367	1.349	20.01	3.047	2.52	– – –	– – –
$\chi 3$ (RL)	1.736	2.58	4.464	46.56	2.606	– – –	– – –
ω (High state)	0.68	1.71	2.532	25.42	2.91	– – –	– – –

[1] kT_{in} : Inner disk temperature.
[2] kT_e : Temperature of the Compton cloud.
[3] τ : Optical depth of the Compton cloud.
[4] Γ_x : Power-law photon index.
[5] RQ : Radio-quiet.
[6] RL : Radio-loud.

"disk-blackbody and a thermal-Compton spectrum" and "disk-blackbody, a power-law and a thermal-Compton spectrum" models to fit the spectra. All the spectral parameters other than the normalizations are fixed for the models which are well-fitted with the data during the radio-quiet low-hard state (class $\chi 2$), radio-loud low-hard state (class $\chi 3$) and the high state of the observations of the class ω. The fitted parameters are shown in Table 5. Comparing the fitted parameters in Table 5, it is observed that the model for the high-soft state of class ω fits better with the spectra during the dip of the class ω (marked as A' in Table 5), soft-dip of class θ and the observation of class δ whereas the $\chi 2$ model fits better with the spectrum of the low-hard dip of class β. From the table, it is also noticed that the spectrum of the observation of class ϕ does not fit any of the models and needs more investigations on the spectral properties of the source. We can draw two important conclusions from the spectral analysis:

- the low soft state seen during class ω, though generically can be classified as spectral state A, it is distinctly different from the long duration spectral state A (class ϕ) and short duration A states seen during class θ etc.
- the spectral shape during the low soft state is similar to the high soft state (with the same set of spectral components).

Hence we can conclude that the high-soft and low-soft states of the observations of class ω do not have any significant difference in the physical parameters of the accretion

Table 5. Spectral parameters during various classes of GRS 1915 + 105.

Model[1]	Normalization[2]	ω_{dip}(A[3])	β_{low}(C[4])	θ_{low}(A[4])	ϕ(A[5])	δ(B[6])
$\chi 2$ (RQ[7])	dbb	351.8	118.5	1605	478.4	2511
	co	3.169	7.835	9.259	1.624	5.824
	Reduced χ^2	9.96	2.71	24.09	37.35	173.7
$\chi 3$ (RL[8])	dbb	13.27	3.6673E-10	38.48	9.710	57.77
	co	0.000	4.8426E-33	0.000	0.000	0.000
	po	0.747	13.97	4.314	2.0348E-33	0.000
	Reduced χ^2	53.39	8.41	27.66	108.46	127.3
ω (RQ)	dbb	81.97	4.6E-25	316.2	103.9	316.2
(High state)	co	4.8E-14	7.5E-25	0.068	0.000	6.8E-02
	po	10.0	27.0	28.63	4.790	28.63
	Reduced χ^2	0.84	135.4	2.02	37.23	2.02

[1] : Model $\chi 2$: Model "Disk-blackbody + CompST" with $kT_{in} = 1.348$ keV, $kT_e = 20.01$ and $\tau = 3.047$
Model $\chi 3$: "Disk-blackbody + Power-law + CompST" with $kT_{in} = 2.580$ keV, $kT_e = 4.464$, and $\tau = 46.56$ and $\Gamma = 2.606$
Model ω : "Disk-blackbody + Power-law + CompST" with $kT_{in} = 1.709$ keV, $kT_e = 2.532$ keV and $\tau = 25.42$ and $\Gamma = 2.912$.
[2] : dbb = Disk blackbody normalization, co = thermal-Compton spectrum normalization, and po = power-law normalization.
[3] : Low-soft state of new class.
[4] : Low-hard state.
[5] : Soft state.
[6] : High-soft state.
[7] : Radio-quiet.
[8] : Radio-loud.

disk of the black hole except the normalization factors and hence these two different intensity states are identical in the spectral and temporal properties of the source and different from the observations of any other reported classes.

4. Discussion

The X-ray observation of Galactic black hole candidates reveal four different spectral states such as

- *"X-ray very high"* state with quite high soft X-ray flux and an ultra-soft thermal of multi-color blackbody spectrum of characteristic temperature $kT \sim 1$ keV and a power-law tail with photon-index $\Gamma \sim 2 - 3$ with approximate X-ray luminosity at Eddington limit,
- *"X-ray high, soft"* state with similar characteristic temperature *kT* and a weak power-law tail but with lower luminosity (by a factor of $\sim 3 - 30$),
- *"X-ray low, hard"* state with a single power-law spectrum with photon-index $\Gamma \sim 1.5 - 2$ with a typical X-ray luminosity of less than 1% of Eddington, and

- *"X-ray off or quiescent"* state with very low level emission with uncertain spectral shape at a luminosity $L_X < 10^{-4}$ of Eddington limit (Grebenev *et al.* 1993; van der Klis 1995). However, it is rare to observe a source exhibiting all the four spectral states.

4.1 *Fast transition between high-soft and low-hard states*

Galactic black hole binaries remain in a canonical spectral state with similar properties for considerably long durations ($\sim$ a few months). This suggests the general stable nature of the accretion disk. Though the microquasar GRS 1915 + 105 shows extended low-hard states as seen in other Galactic black hole candidates, the state transition between the low-hard state and high-soft state occurs in a wide range of time scales. Attempts have been made to explain the observed state transitions when the source shows regular periodic bursts in the X-ray light curves. Belloni *et al.* (1997) have tried to explain the repeated patterns (burst/quiescent cycle) in the X-ray light curve as the appearance and disappearance of the inner accretion disk. They have shown that the outburst duration is proportional to the duration of the previous quiescent state. Taam *et al.* (1997) have attempted to describe these transitions in the framework of thermal/viscous instabilities in the accretion disk. They have argued that the geometry of the accretion disk in GRS 1915 + 105 consists of a cold outer disk extending from radius $r_{in} \sim 30$ km to infinity and a hot, optically thin inner region between $r = 3$ km and r_{in}. They have interpreted the spectral changes between low-hard and high-soft states as arising due to the change in the value of inner disk radius. Nayakshin *et al.* (2000) tried to explain the observed temporal behavior of GRS 1915 + 105 invoking the model of standard cold accretion disk with a corona that accounts for the strong nonthermal X-ray emission and plasma ejections in the jet when the source luminosity approaches the Eddington limit. This model qualitatively explains the observed cyclic features in the light curves (classes ρ, α, and λ), the dependence of the overall evolution and the values of the cycle times on the time-averaged luminosity, and the fact that the transitions between the states can be very much shorter than the corresponding cycle time. This model also successfully explains the ejections of plasma into radio jets and the associated dip features (class β) seen in the X-ray light curves of the source.

Rao *et al.* (2000) have observed a slow transition from an extended low-hard state to a high-soft state ($\sim$ 3 months) in 1997 March−August. Fast transition (a few seconds) between the two spectral states is observed during many occasions when the source exhibits irregular bursts (Rao *et al.* 2000), soft dips (Naik *et al.* 2001) in the X-ray light curves. Chakrabarti *et al.* (2000) interpreted the observed spectral transition in GRS 1915 + 105 in the light of advective disk paradigm which includes self-consistent formation of shocks and out-flows from post-shock region. The observed fast transition between the two canonical spectral states implies the solutions for the accretion disk during two states exist for similar net (i.e., sum of the Keplerian and sub-Keplerian) $\dot{m}$. This is because the time scale of fast transition ($\sim$ 10 s) is not sufficient for the readjustment of the accretion disk at the outer edge to create a significant change in $\dot{m}$.

4.2 *Fast transition between high-soft and low-soft states*

The Galactic microquasar GRS 1915 + 105 remains in the low-hard state for extended periods and switches from the low-hard state into a high-soft state in a wide range of

time-scales. During the low-hard state, the source spectrum is dominated by the non-thermal component and the inner edge of the accretion disk lies far away from the black hole event horizon. However, during the high-soft state, the spectrum is dominated by the thermal component and the inner edge of the accretion disk extends towards the event horizon. The Compton cloud which is responsible for the Comptonization of the soft X-ray photons during the low-hard state vanishes during the high-soft state. The X-ray flux has a significant contribution from the non-thermal component during the low-hard state whereas the thermal component is dominated over by the non-thermal component during the high intensity soft states. The transition between the above two canonical spectral states takes place because of the infall of matter from the inner accretion disk into the black hole and presence and absence of the Compton cloud. However, the observed transition between the high-soft and low-soft states (present work) without any significant change in the geometry of the accretion disk is interesting new phenomenon. We try to explain this observed feature invoking a model where the viscosity parameter of the accretion disk is very close to the critical viscosity.

We observed a factor of ~ 3.5 difference in the X-ray flux in 2 – 60 keV energy range during the high-soft (non-dip) and low-soft (dip) states of class ω. If this could be due to the decrease in the mass accretion rate, according to ADAF, the source spectrum during this low intensity state should be hard which is not the case. The softness of the source spectrum during the low state (dip) of class ω makes it clear that the observed change in intensity during these states (dip and non-dip) cannot be due to the change in mass accretion rate at the outer edge. Although similar change in X-ray flux during the dip and non-dip regions was observed in the light curves of the black hole candidates GRO J1655–40 and 4U 1630–47 (Kuulkers *et al.* 1998), these dips are different from those observed in GRS 1915 + 105. In earlier cases, the source spectra during the dips were heavily absorbed by some intervening material. The spectra during the dips when fitted by a model with power law and absorbed disk blackbody as the model components, the equivalent hydrogen column densities (N_H) for the two sources were found to be $27 \times 10^{22}\,\mathrm{cm}^{-2}$ and $34 \times 10^{22}\,\mathrm{cm}^{-2}$ respectively which are about one order higher in magnitude than the interstellar absorption column densities ($N_{H_{\mathrm{int}}}$). The values of N_H were very high ($\geq 76 \times 10^{22}\,\mathrm{cm}^{-2}$) for both the sources when the spectra were fitted with a model with blackbody and absorbed disk blackbody as model components. However, the source spectra during the dips (low-soft state) in GRS 1915 + 105 are well described by "disk blackbody, power law and a thermal Compton-spectrum" model without any absorbing medium other than $N_{H_{\mathrm{int}}}$. Hence, the decrease in X-ray intensity during the dips cannot be explained by absorption by the intervening medium. As the source is radio-quiet during the observations of this class, the decrease in X-ray intensity cannot be explained by the evacuation of matter from the accretion disk which causes flares in radio and infrared bands.

The observed unusual transition between two different intensity states in GRS 1915 + 105 is attributed to the change in the temperature of the inner accretion disk without incorporating any significant change in the inner radius. The inner accretion disk during the high intensity state (non-dip) is hotter than the low intensity state (dip). The duration of the observed dips and non-dips are in the range 20 – 95 s and 200 – 550 s. If the variation in the intensity between two dips and non-dips are due to the emptying and replenishing of the inner accretion disk caused by a viscous thermal instability, then the viscous time can be explained by (Belloni *et al.* 1997)

$$t_{\rm vis} = 30\alpha_2^{-1} M_1^{-1/2} R_7^{7/2} \dot{M}_{18}^{-2} s \tag{1}$$

where $\alpha_2 = \alpha/0.01$, R_7 is the radius in units of 10^7 cm, M_1 is the mass of the compact object in solar masses, and $\dot{M}_{18}$ is the accretion rate in units of 10^{18} g s^{-1}. Using all these parameters, Belloni *et al.* (1997) found that the model agrees with the data with a relation of the form $t_q \propto R^{7/2}$, where t_q is the time interval for the quiescent phase. Applying the values of the radius of the inner accretion disk during the dip to the above expression, the duration of the derived quiescent (dip) period does not match with the observed dip duration. These results manifest that the above model cannot explain the the observed transition between two intensity states.

We attempt to explain the observed phenomenon of state transition between different intensity states in GRS 1915 + 105 by invoking the two component advective flow (TCAF) model of Chakrabarti & Titarchuk (1995) which consists of two major disk components

- standard, optically thick disk component produced from the Keplerian or the sub-Keplerian matter at the outer boundary and
- quasi-spherical and axisymmetric sub-Keplerian halo component.

The advantage of this model is that the soft and hard X-ray radiations are formed self-consistently from the same accretion disk without invoking any adhoc components such as the plasma cloud, hot corona, etc. whose origins have never been clear. According to this model, the temperature of the Keplerian disk increases with the increase in the accretion rate of Keplerian disk. The increase in the number of soft photons intercepted by the post-shock region results in reducing its temperature. Assuming Comptonization as the dominant mechanism for cooling, the expression for the electron temperature T_e can be given as

$$T_e = \frac{T_{es} r_s}{r} e^{C_{\rm comp}(r^{3/2} - r_s^{3/2})} \tag{2}$$

where $C_{\rm comp}$ is a monotonically increasing function of optical depth assuming a constant spectral index, r_s is the shock location and T_{es} is the electron temperature at r_s. For $C_{\rm comp} > r_s^{-3/2}$, the cooling due to Comptonization overcomes geometrical heating and T_e drops as the flow approaches the black hole. According to this model, a disk with completely free (Keplerian) disk and (sub-Keplerian) halo accretion rates for a black hole of mass $M = 5M_\odot$, exhibits multiplicity in spectral index (when both the rates are fixed) or multiplicity in disk accretion rate when the spectral index is similar (see, Fig. 3a of Chakrabarti & Titarchuk, 1995). In the observation described in this paper, there is no evidence for a large variation of the spectral index. This signifies that though there is not enough time for a change in the total rate (as the transition between the high-soft and low-soft states takes place within a time range of ≤ 10 s), individually, Keplerian and sub-Keplerian rates may have been modified. This is possible if the Shakura-Sunyaev viscosity parameter α is very close to the critical value ($\alpha \sim \alpha_c \sim 0.015$; Chakrabarti 1996). When α of the entire disk is well above α_c, the entire disk is pretty much Keplerian, except very close to the black hole ($r < 3r_g$, where r_g is the Schwarzschild radii). Similarly when α of the entire flow is well below α_c, the flow is sub-Keplerian with a possible standing or oscillating shock wave (Chakrabarti 1996). Since viscosity in a disk can change in a very small time

scale (convective/turbulent time-scale in the vertical direction) it is not unlikely that the viscosity near the Keplerian-disk surface is very close to the critical value during the time when this new class is exhibited. The high-intensity state will then correspond to the ordinary Keplerian disk. Extraordinary laminary flow may reduce viscosity at some stage, and sub-Keplerian flow develops out of the Keplerian disk both above and below the Keplerian disk. This sub-Keplerian flow need not be hotter since excess soft photons from the underlying Keplerian disk cools it instantaneously. Temperature and intensity of the radiation from the Keplerian disk drops to the point that a thin outflow develops from the sub-Keplerian flow. This is the low intensity state. This wind is cooled down and is fallen back on the Keplerian disk, increasing the Keplerian rate, intensity and viscosity, thereby cutting off the wind and bringing the flow to the high intensity state again. Unlike the transition from State B to State C (as described by Belloni *et al.* 2000 and explained in Chakrabarti *et al.* 2000), where the sub-Keplerian flow may always be present, in the present case, the high intensity state need not have a sub-Keplerian component at all. The transition from one soft-state to another could in fact be due to the interesting change in topology of the flow at the critical viscosity.

5. Acknowledgements

Work of SN is partially supported by the Kanwal Rekhi Scholarship of the TIFR Endowment Fund. We thank the RXTE, BATSE, and NSF-NRAO-NASA GBI team for making the data publicly available. This research has made use of data obtained through the High Energy Astrophysics Science Archive Research Center Online Service, provided by the NASA/Goddard Space Flight Center. The Green Bank Interferometer is a facility of the National Science Foundation operated by the NRAO in support of NASA High Energy Astrophysics programs.

References

Belloni, T., Mendez, M., King, A. R., *et al.* 1997, *Ap. J.*, **488**, L109.
Belloni, T., Klein-Wolt, M., Mendez, M. *et al.* 2000, *A&A*, **355**, 271.
Castro-Tirado, A. J., Brandt, S., Lund, N. 1992, *IAU Circ.*, 5590.
Chen, X., Swank, J. H., Taam, R. E. 1997, *Ap. J.*, **477**, L41.
Chakrabarti, S.K., 1996, *Ap. J.*, **464**, 664.
Chakrabarti, S.K., Manickam, S.G., Nandi, A. *et al.* 2000, submitted to World Scientific (astro-ph – 0012525)
Chakrabarti, S.K., Titarchuk, L.G. 1995, *Ap. J.*, **455**, 623.
Grebenev, S.A., Sunyaev, R., Pavlinsky, M. *et al.* 1993, *A&AS*, **97**, 281.
Greiner, J., Morgan, E. H., Remillard, R. A. 1996, *Ap. J.*, **473**, L107.
Klein-Wolt, M., *et al.* 2002, MNRAS, (astro-ph/0112044)
Kuulkers, E., Wijnands, R., Belloni, T. *et al.* 1998, *Ap. J.*, **494**, 753.
Mirabel, I. F., Rodriguez, L. F. 1994, *Nat.*, **371**, 46.
Mirabel, I. F., Dhawan, V., Chaty, S. *et al.* 1998, *A & A*, **330**, L9.
Morgan, E.H., Remillard, R.A., Greiner, J. 1997, *Ap. J.*, **482**, 993.
Muno, M.P., Morgan, E.H., Remillard, R.A. 1999, *Ap. J.*, **527**, 321.
Naik, S., Rao, A.R. 2000, *A&A*, **362**, 691.
Naik, S., Agrawal, P.C., Rao, A.R. *et al.* 2001, *Ap. J.*, **546**, 1075.
Naik, S., Agrawal, P.C., Rao, A.R., Paul, B. 2002, *MNRAS*, **330**, 487.
Nayakshin, S., Rappaport, S., Melia, F. 2000, *Ap. J.*, **535**, 798.
Rao, A.R., Yadav, J.S., Paul, B. 2000, *Ap. J.*, **544**, 443.
Smith, D.M., Heindl, W.A., Markwardt, C.B., Swank, J.H. 2001, *Ap. J.*, **554**, L41.

Taam, R.E., Chen, X., Swank, J.H. 1997, *Ap. J.*, **485**, L83.
van der Klis, M. 1995, in *X-ray Binaries*, (ed.) W. Lewin, J. van Paradijs, & E. van den Heuvel (Cambridge: Cambridge Univ. Press) 252.
Zdziarski, A.A., Grove, J.E., Poutanen, J., *et al.* 2001, **554**, L45